An Improved Method to Estimate Savings from Thermal Comfort Control in Residences from Smart Wi-Fi Thermostat Data

Abdulelah D. Alhamayani

Qiancheng Sun

Kevin P. Hallinan (0000-0002-0305-4886)

Article

An Improved Method to Estimate Savings from Thermal Comfort Control in Residences from Smart Wi-Fi Thermostat Data

Abdulelah D. Alhamayani *, Qiancheng Sun and Kevin P. Hallinan *

Department of Mechanical & Aerospace Engineering, University of Dayton, Dayton, OH 45469-0238, USA; sunq11@udayton.edu

* Correspondence: alhamayania1@udayton.edu (A.D.A.); kevin.hallinan@udayton.edu (K.P.H.)

Abstract: The net-zero global carbon target for 2050 needs both expansion of renewable energy and substantive energy consumption reduction. Many of the solutions needed are expensive. Controlling HVAC systems in buildings based upon thermal comfort, not just temperature, uniquely offers a means for deep savings at virtually no cost. In this study, a more accurate means to quantify the savings potential in any building in which smart WiFi thermostats are present is developed. Prior research by Alhamayani et al. leveraging such data for individual residences predicted cooling energy savings in the range from 33 to 47%, but this research was based only upon a singular data-based model of indoor temperature. The present research improves upon this prior research by developing LSTM neural network models for both indoor temperature and humidity. Validation errors are reduced by nearly 22% compared to the prior work. Simulations of thermal comfort control for the residences considered yielded potential savings in the range of 29–43%, dependent upon both solar exposure and insulation characteristics of each residence. This research paves the way for smart Wi-Fi thermostat-enabled thermal comfort control in buildings of all types.

1. Introduction

The Intergovernmental Panel for Climate Change (IPCC) has set a target of net-zero carbon emissions by 2050 [1]. To get there, the International Energy Agency (IEA) estimates that clean energy investment by 2030 must increase three-fold to USD 4 trillion [2]. Technology innovation is certain to comprise a sizeable part of this investment [3]. One of the recent technologies proven to reduce the global energy demand are smart thermostats. In Europe, this technology, which has been adopted in over 1 million residences, has demonstrated 22% energy savings in this sector. If applied to all residences in Europe, total European carbon dioxide (CO_2) emissions can be reduced by around 5% [4]. Likewise, the US Government has incentivized purchase of this technology for residences [5]. To date, 17% of residences in the US now have such thermostats installed [6].

One application of smart Wi-Fi thermostats that has been identified is for use in controlling for thermal comfort rather than temperature. Several researchers have reported potential cooling energy savings from thermal comfort-driven and energy-aware HVAC system control ranging from 4 to 32% in commercial buildings [7–10]. Ferreira et al., applying neural network-based model for predictive thermal comfort control in a commercial building, reported even greater estimated energy savings of more than 50% [11].

In residential buildings, Danassis et al. implemented artificial neural network and Fuzzy Logic inference models to assess smart thermostat thermal comfort control. They estimated savings in the range of 18–40% [12]. Likewise, Lou et al. showed potential cooling savings from similar control of up to 85% for a one-month period in the summer in

the Midwest, US [13]. Lastly, Alhamayani et al. expanded Lou et al.'s effort by accounting for the influence of solar heat gain. They showed that solar contributions to cooling were significant. They reported more realistic cooling energy savings in the range of 33–47%. Further, they showed that the extent of the savings clearly depended upon the amount of insulation in a residence and exterior shading from other buildings and from trees [14]. A very recent study by Sun et al. [15] demonstrated solar heat gain to the same housing set considered by Lou et al. [13] and Alhamayani et al. [14] is responsible for up to 72% of the cooling load in the residences considered [15].

The promise of implementing thermal comfort control in residences is increasing, especially with the global market for manufacturing smart thermostats predicted to increase from USD 88.7 billion to USD 228.2 billion from 2021 to 2027 [16]. This is expected to translate to an estimated 1-2B new smart Wi-Fi thermostats entering the market. Such a gain in the market coupled with implementation of thermal comfort control could yield substantial worldwide carbon reduction at virtually no cost.

The objective of this study is to build upon the prior research of Alhamayani et al. [14] to further improve the accuracy of estimation of the energy savings from implementing smart thermostat thermal comfort control in residences. In comparison to the prior work of Lou et al. [13] and Alhamayani et al. [14], which assumed a constant indoor relative humidity of 55%, this study accounts for this influence. The improvement in temperature and relative humidity models is discussed. The impact of the addition of a relative humidity model to the estimation of the PMV value is documented. The estimated energy savings from the current study is compared to the previous work by Alhamayani et al. [14].

2. Background

In general, residential and commercial buildings HVAC maintain human thermal comfort through the maintenance of a set indoor temperature. However, human thermal comfort depends on a number of other factors, including (i) other indoor environmental factors (relative humidity, air velocity, and mean radiant temperature, MRT); and (ii) occupational factors (occupants' age, gender, clothing, metabolic rate, and behavior, such as turning on/off the a/c or opening or closing windows) [17].

The well-known model utilized to quantify the thermal comfort of an occupant inside a controlled space is Fanger's predicted mean vote (PMV). The PMV model generally estimates the mean value of votes of occupants using a seven-point thermal sensation scale, ranging from −3 (much too cold) to +3 (much too hot). The optimal PMV range, as suggested in the ASHRAE 55 and ISO 7730 standards, is from −0.5 to +0.5 [18].

Prior research estimating savings from thermal comfort control in residences has relied upon different control strategies and algorithms. Azuatalam et al. [19] leveraged a reinforcement learning agent to control the heating, ventilation, and air conditioning (HVAC) system in a commercial building. The power reduction realized from their control strategy reached a maximum of 50% weekly. Further, Park et al. [20] utilized a thermal comfort-based controller to reduce the cooling energy of air-conditioning systems in a residential building in Kuwait. Energy savings of 39.5% on a representative summer day were documented. Another developed control strategy developed by Li et al. [21] based on PMV-PDD smart thermostat control showed savings in a residential building of up to 11.5%.

The use of smart Wi-Fi PMV-based thermal comfort control is new. Only Lou et al. [13] and Alhamayani et al. [14] are the only known efforts that have relied upon this technology. Thus, in what follows in the results section, comparisons are made only with this prior work.

The proposed study here extends the prior work reported in Alhamayani et al. [14], following the framework established by Bac et al. [22], which posed a process for identifying suitable HVAC system options for a building by using building energy simulations. Here, these simulations are based upon data-based models of the energy systems. This prior work of Alhamayani et al. relied upon a data-based machine learning model using archived smart thermostat data in addition to outdoor weather conditions and solar heating inputs

to predict internal temperature. The developed model was utilized to estimate a residence's PMV and control the cooling load to achieve the optimal PMV at all times. The developed model considered the overall solar heat gain through the building envelope and from solar fenestration. However, as noted in Section 1, the prior research by Alhamayani et al. utilized an assumption of constant internal relative humidity (set to 55%). This paper again leverages archived smart Wi-Fi thermostat data (internal temperature and relative humidity and cooling status). It relies upon these data to develop data-based machine learning models to predict both the internal temperature and relative humidity. It then integrates these models into a simulated thermal comfort control schema to evaluate more accurately the thermal comfort control for several residences with variable solar exposure and building envelope energy effectiveness. As a result, the predicted savings estimates from thermal comfort control will be more realistic.

The remainder of the paper presents the methodology for developing a database machine learning model for both the internal temperature and relative humidity. It then employs the developed models into a simulated control of thermal comfort in several residences with variable solar exposure and energy effectiveness. It concludes with a discussion of the results and implications of this research.

3. Methodology

3.1. Data Collection

3.1.1. Buildings, Smart Thermostats, Weather, and Solar Data

All the building characteristics, smart thermostats, weather, and solar data used in the earlier work by Lu et al. [13] and Alhamayani et al. [14] are utilized here. Table 1 documents the building characteristics of the residences used in this study.

Table 1. Residential building geometrical and energy characteristics data.

Home Characteristics/House No.	1	2	3	4	5
A_{floor} (m^2)	54	84	54	59	45
A_{wall} (m^2)	159	187	156	152	149
A_{window} (m^2)	2–3	2–3	2–3	2–3	2–3
R_{wall} (m^{2}KW^{-1})	0.88	0.7	0.7	2.5	0.8
R_{window} (m^{2}KW^{-1})	0.35	0.35	0.35	0.35	0.35
R_{Attic} (m^{2}KW^{-1})	3.87	2.15	1.1	6.69	3.17
AC power (kW)	10.5	8.8	10.5	10.5	12.25

3.1.2. Smart Thermostats Moving Averages

Prior work by Alhamayani et al. [14], Huang et al. [23], Sun et al. [15], and Lou et al. [13] developed models from archived time smart Wi-Fi measurements. The analysis described here uniquely considers possible inputs to the model described in Section 3.1.2, moving averages of the smart Wi-Fi measured indoor temperature and relative humidity, as well as the cooling demand status. The smoothing effect of using a moving average can improve the prediction accuracy of machine learning models [24,25]. Different averaging window time intervals were considered for each of the major features (indoor temperature, indoor humidity, and cooling demand status). An optimal moving average window associated with the lowest validation error from the models developed was determined for each residence. This ranged from 1 to 7 h, with the lower range associated with poor energy effectiveness residences and the larger range associated with high energy effectiveness houses. Table 2 lists the optimal interval moving averages for the selected features for each residence in this study.

Table 2. List of the optimal interval moving averages for the selected features for each residence.

House Number	Moving Average Period for Temperature (h)	Moving Average Period for Relative Humidity (h)	Moving Average Period for Cooling Demand (h)
1	4	3	2
2	4	5	1
3	3	2	1
4	7	5	1
5	4	6	1

3.1.3. Data Preprocessing and Feature Engineering

The data pre-processing required here consisted of (i) creating uniformly spaced thermostat data from the actual event-based data. The thermostat data were archived only when one of the measured features changed values. Additionally, the hourly weather and solar data were synched with these data using linear interpolation. This data pre-processing was described in earlier work [14].

In addition, Pearson's correlation method was applied to eliminate highly correlated features (r > 0.9) [26]. Min–max normalization was applied as well. Sample smart Wi-Fi thermostat features for one of the residences are shown in Table 3.

Table 3. Sample of synchronized Smart Wi-Fi thermostat, weather, and moving averages features for relative humidity model.

Indoor Relative Humidity (%)	Outdoor Temperature (F)	Outdoor Dew Point Temperature (F)	Cooling Setpoint Temperature (F)	Cooling Demand Status (0/1)	Moving Average Relative Humidity (%)	Moving Average Indoor Temperature (F)	Moving Average Cooling Demand (0–1)
61	79	70	75	0	61	74.7	0
54	78	65	75	0	53.8	75.5	0.2
56	83	66	72	1	58.8	72.1	0.53

3.2. Temperate and Relative Humidity Models Development

Long Short-Term Memory (LSTM)

In this study, a deep learning neural network algorithm was considered for developing two separate dynamic models to predict the indoor temperature and relative humidity using archived smart Wi-Fi thermostat data. The deep learning neural network developed employed the long short-term memory (LSTM) neural network algorithm introduced by Hochreiter and Schmidhuber in 1997 [27]. The LSTM is a type of recurrent neural network (RNN). Much prior work has validated that LSTM performs better than RNN by overcoming the gradient vanishing problem or gradient explosion problem by forgetting the previous observations having little influence over current predictions [27–30].

The architecture of the LSTM can be summarized as a combination of three types of gates (forget gate, input gate, and output gate). LSTM advantages gates to add or remove information to the cell state [26]. The equation for all gates (forget f_t, input i_t, and output o_t) are:

$$f_t = \sigma\left(W_f[h_{t-1},\ x_t] + b_f\right) \tag{1}$$

$$i_t = \sigma(W_i[h_{t-1},\ x_t] + b_i) \tag{2}$$

$$o_t = \sigma(W_o[h_{t-1},\ x_t] + b_o) \tag{3}$$

The cell state C_t equation is:

$$\widetilde{C}_t = \tanh(W_c[h_{t-1}, x_t] + b_C) \tag{4}$$

$$C_t = f_t * C_{t-1} + i_t * \widetilde{C}_t \tag{5}$$

The output h_t that comes out from the LSTM unit is:

$$h_t = o_t * \tanh(C_t) \tag{6}$$

Generally, LSTM utilizes prior readings or values for all features (including the response variable) as predictors for the next response prediction by considering a lookback period that controls the time period of prior readings or values used to forecast the next response time step. To achieve the most effective predictive models and prevent overfitting issues, as well as speed up the computations, the data are batched. The batch size controls the number of training samples applied in one iteration and enables the propagation of weightings across time.

The data used for model development, validation, and testing were split sequentially according to 72%/18%/10%. The batch size was set to be 128 in both models. Model performance was assessed utilizing R-squared (R^2), mean absolute error (MAE), mean absolute percentage error (MAPE), and root mean square error (RMSE).

3.3. The Effect of Multiple Predictive Models on PMV
Predictive Mean Vote (PMV) Model

The quantification of thermal comfort in this study is obtained by "Fanger's predicted mean vote (PMV) model" [17]. The levels of comfort are well defined in the seven-point thermal sensation scale proposed by the American Society of Heating, Refrigerating, and Air-Conditioning Engineers (ASHRAE). The thermal sensation scale is: −3 (Cold), −2 (Cool), −1 (Slightly cool), 0 (Neutral), +1 (Slightly warm), +2 (Warm), and +3 (Hot); and it represents the thermal sensation of a majority of people. A PMV index range between −0.5 and +0.5 is most satisfactory to 80% of people [31].

The following values were set for the required parameters in the PMV calculation. The metabolic rate, M, was set to range from 1 to 1.3 met, applicable to a residential activity. The clothing insulation value, I_{cl}, was set to range from 0.45 to 0.5 in the summer. The relative air velocity term, var, was equated to range from 0.1 to 0.2 m/s, based upon the minimum value accepted by ASHRAE-55 [18]. The next subsections detail the estimation and validation of the MRT, respectively. Future work could potentially relax these assumptions.

The flowchart shown in Figure 1 summarizes how thermal comfort control was enhanced from earlier work [14] and simulated in the housing set described in Table 1. It is clear the relative humidity model has been added to the thermal comfort control logic to add more realistic PMV estimates to the previous work.
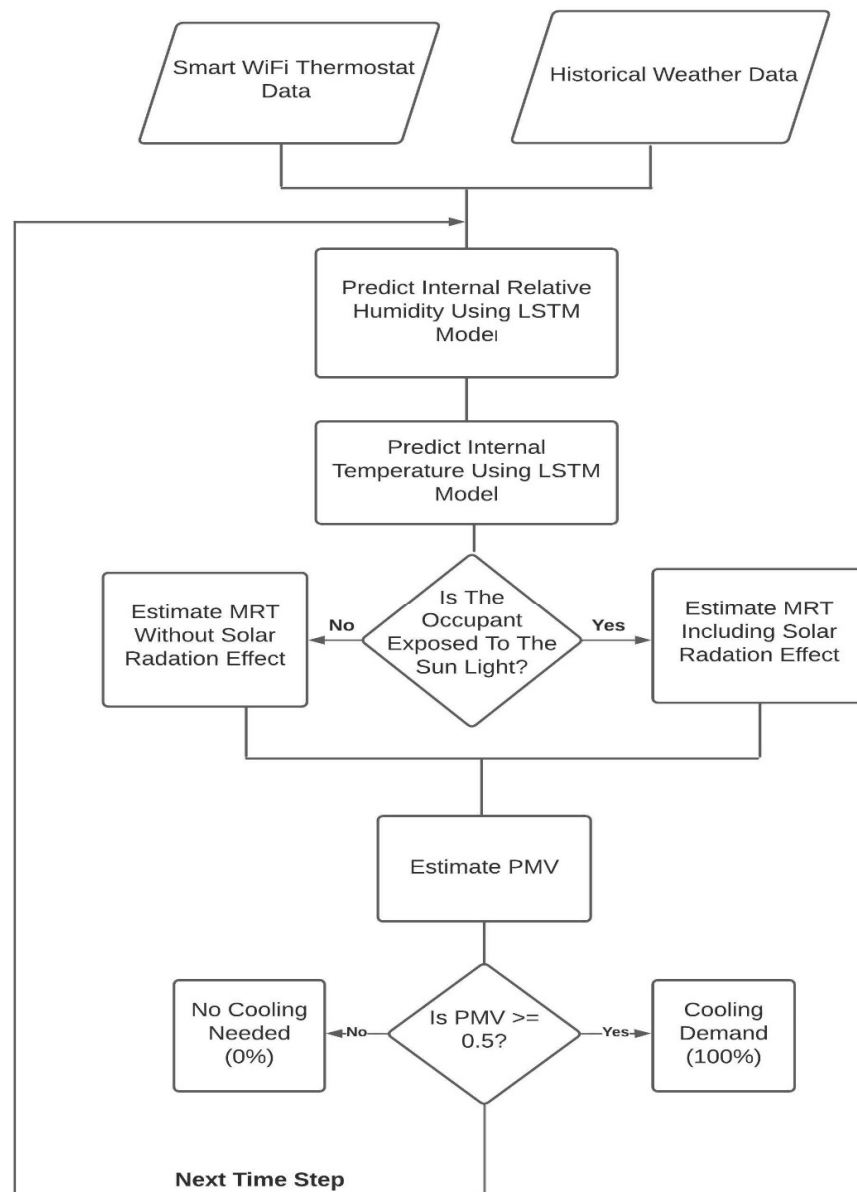
Figure 1. Flowchart showing process for simulated thermal comfort control using two developed LSTM deep learning neural network models of internal relative humidity and temperature.

3.4. Potential Savings from PMV Control Utilizing Two Predictive Models

The potential savings from thermal comfort control was determined by comparing the simulated cooling using thermal comfort control to the actual cooling. The energy savings were determined by considering the effective duty cycle for the whole period and the cooling size of the residence's HVAC, where the cooling duty cycle is defined as:

$$Effective\ Duty\ Cycle = \frac{\sum (Cooling\ time) \times (Cooling\ Demand\ Status)}{\sum Time} \qquad (7)$$

4. Results

Results are presented to provide evidence that the use of two data-based models for indoor temperature and relative humidity, coupled with the use of time-averaged quantities for internal temperature, internal relative humidity, and cooling demand status, improves the estimation of savings from PVM-based thermal comfort control relative to prior work done by Alhamayani et al. [14].

4.1. Model Performance and Validation Results

Models for the moving average thermostat temperature and humidity were developed using the Adam optimization algorithm [32]. Different neural network architectures were considered. Two hidden layers with 25–30 and 10–20 neurons were tested. Additionally, different lookback time steps (15–20 time steps) were considered. The validation error metrics (R^2, MAE, MAPE, and RSME) were used to identify the best values for these hyperparameters. Table 4 lists the optimum hyper-parameters and the validation metrics for the two models. Noteworthy is the MAE of 0.317 for temperature model validation. This represents a significant improvement relative to the prior work of Alhamayani et al., for which the MAE was 0.406 [14]. Clearly, the addition of the internal humidity as a predictor for temperature and use of moving averages of temperature, relative humidity, and cooling demand status clearly improved the model.

Table 4. Hyper-parameters and the validation metrics for the relative humidity and temperature models.

Model	Lookback Steps	Hidden Layers (Units)	Batch Size	MAE	R^2	MAPE (%)	RSME
Relative humidity	15	25	10	128	0.3694	0.9540	0.6709	0.6793
Temperature	20	30	15	128	0.317	0.9551	0.4256	0.4455

Figure 2 presents a time series plot of the measured internal relative humidity and the predicted internal relative humidity over the time period of 2 June 2018–24 June 2018 for House #1. Included in this figure are the actual humidity value (black color), the predicted humidity value for training (deep pink color), and the predicted humidity value for validation (blue color) and testing data (dark violet color). There is excellent correspondence between the predicted humidity and the actual humidity in the validation and testing ranges.
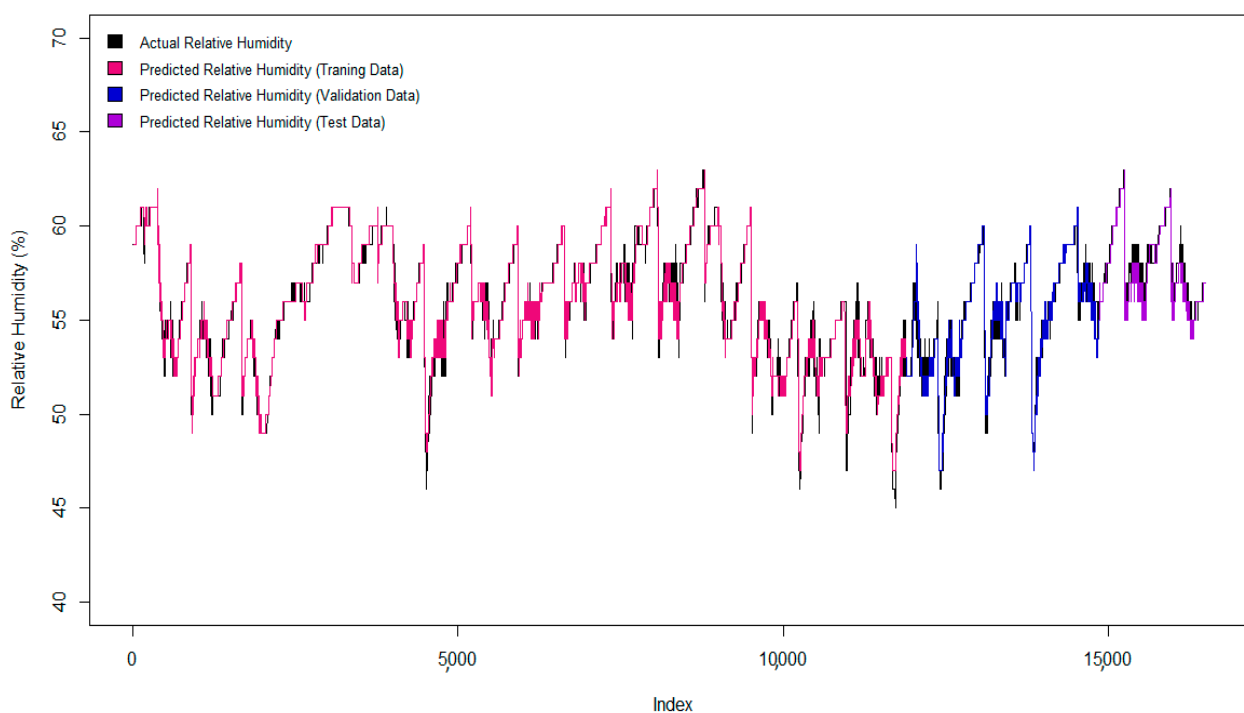

Figure 2. Actual relative humidity versus predicted relative humidity for the whole dataset using an LSTM model with including moving averages of some features.

Figure 3 shows a similar plot for the enhanced temperature model, which uses as an input the relative humidity. Included in this figure are plots of the measured temperature data (black color), and the predicted temperature data for the training (blue color), testing (green color), and validation (red color) data. The correspondence between the measured data and the predictions in the validation and testing ranges is strikingly better than the previous work of Lou et al. [13], Huang et al. [23], and Alhamayani et al. [14].
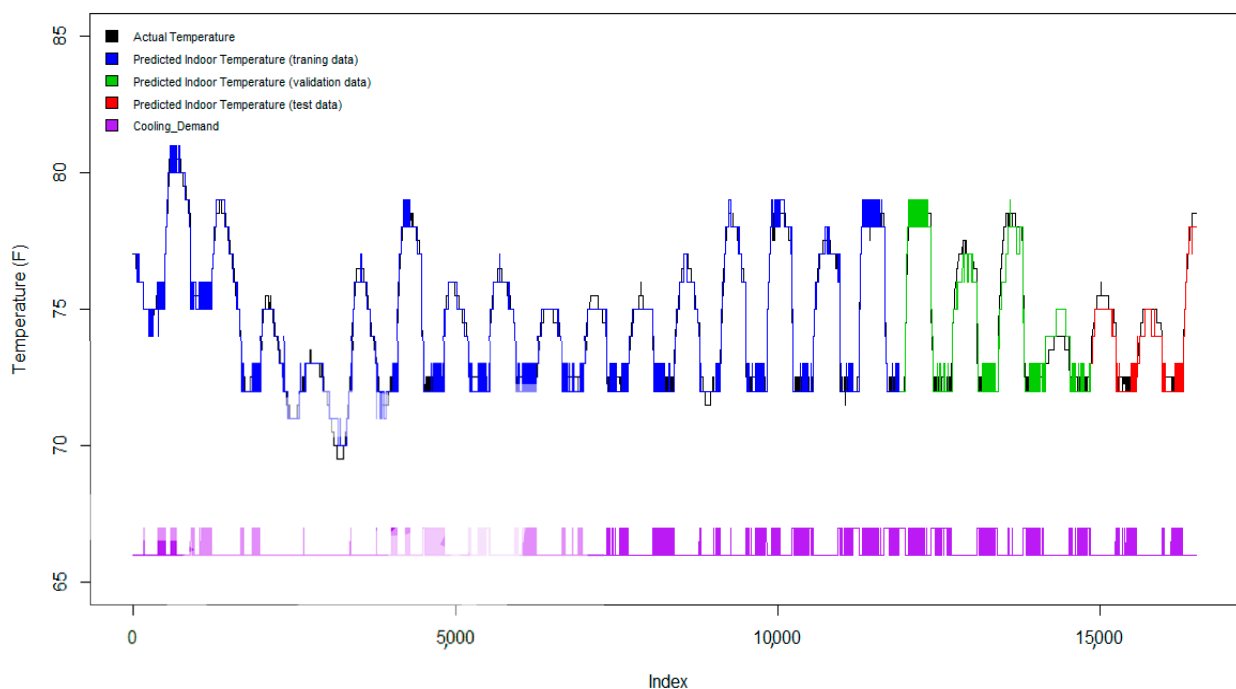

Figure 3. Actual temperature versus predicted temperature for the whole dataset using an LSTM model obtained using the indoor relative humidity and moving averages as features.

Other considered residences detailed in Table 1 show similar results, as documented in Table 5. As seen in this table, the MAE values for each of the residences considered range from 0.317 to 0.412.

Table 5. Validation matrices for all residences' models.

House No.	MAE	R^2	MAPE (%)	RSME
1	0.317	0.9551	0.4256	0.4455
2	0.319	0.9512	0.4313	0.4577
3	0.349	0.9457	0.4730	0.5230
4	0.396	0.9398	0.5285	0.5752
5	0.323	0.9498	0.4402	0.4607

Figure 4 presents a time series of the PMV values estimated for two cases: (a) a constant relative humidity of 55% all over the time period, and (b) a relative humidity predicted using the developed machine learning model for indoor humidity. The plot represents a humid day in Dayton, Ohio, and demonstrates how the relative humidity affects the PMV estimations. It is clear that the more realistic higher relative humidity obtained here causes the PMV index estimation during the day (orange line) to be greater than the constant relative humidity case considered by Alhamayani et al. [14]. Also shown is that for the more realistic relative humidity model, additional cooling is required (see purple cooling demand status) in comparison to the case where a constant relative humidity is assumed. Thus, the model improvement almost certainly yields a more realistic perspective of the potential savings from PMV thermal comfort control relative to typical temperature control of thermal comfort.
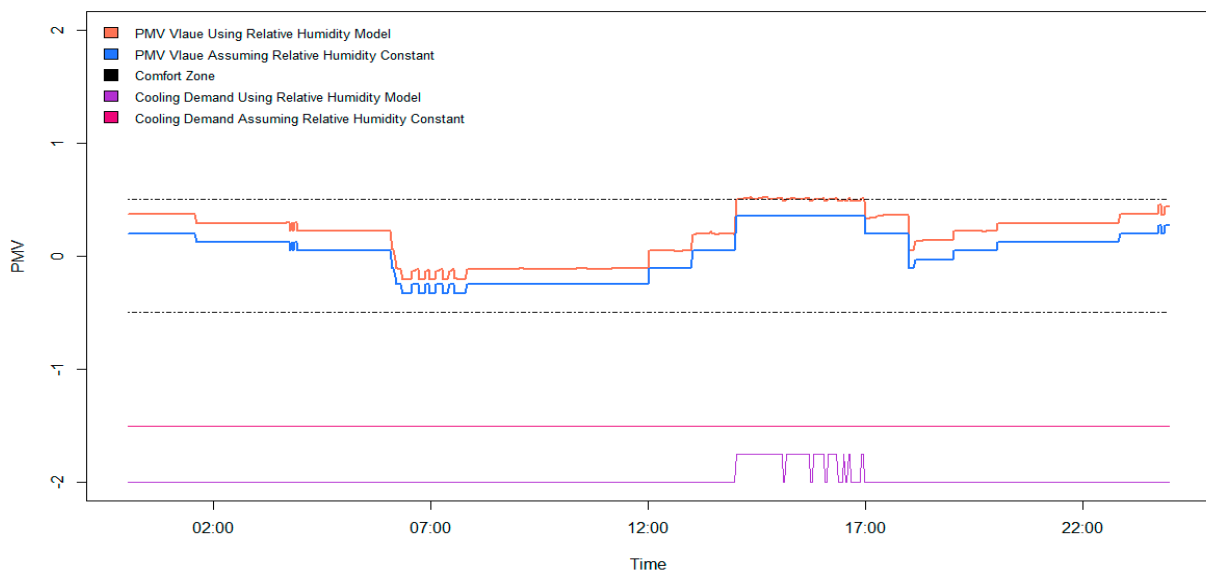
Figure 4. Time series plot of real-time PMV value and cooling demand for the including relative humidity model and assuming relative humidity as constant value.

4.2. Potential Savings from PMV Control Utilizing Current Approach Reliant upon Both a Temperature and Humidity Predictive Model as Compared to Previous Approach Reliant upon Only a Predictive Model for Temperature

Figure 5 presents a comparison of the total cooling energy consumption for each of the eight residences over the time period from 2 June 2018 to 24 June 2018 for two cases: (i) thermal comfort control using only a predictive model for temperature (the demonstrated results were taken from the previous work done by Alhamayani et al. [14]); and (ii) thermal comfort control using two predictive models (relative humidity and temperature). The blue bars represent the cooling energy consumption for case (i), while the red bars represent the cooling energy consumption for case (ii). It is clear that the addition of a humidity model yields greater cooling energy consumption in comparison to similar predictions based upon an assumed constant indoor relative humidity.
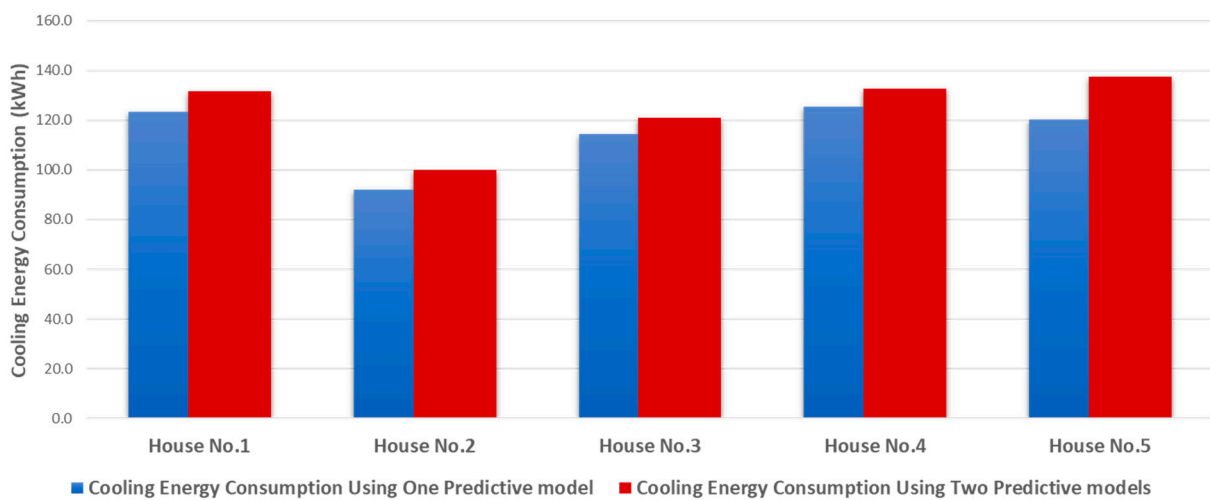

Figure 5. Cooling energy consumption for the residences described in Table 1 for two cases: (1) PMV control with one predictive model (temperature) (Alhamayani et al. [14]) and (2) PMV control with two predictive models (relative humidity and temperature).

Figure 6, which shows lines chart for the relative humidity measured in selected residences over the time period covered, sheds some light on the differences seen in Figure 5. Also included in this plot is the outdoor relative humidity. It is shown that the indoor relative humidity tends to a damped tracking of the outdoor relative humidity. Notable is that one of the buildings (House No. 7) generally has lower relative humidity values than the other houses. The reason for this is likely because the air leakage in this newer residence designed to Energy Star criteria is significantly lower. It is certain that the thermal comfort experienced by residents during this time period was negatively influenced by indoor humidity as the simulated relative humidity is greater than the 55% constant value assumed in the prior study. Subsequently, the energy savings from thermal comfort control are lower than was predicted from the previous work done by Alhamayani et al. [14], as documented for each of the residences in Table 6. The energy savings from thermal comfort control for the residences considered ranged from 29 to 43%, in contrast to savings ranging from 33 to 47% in the prior work by Alhamayani et al. [14].
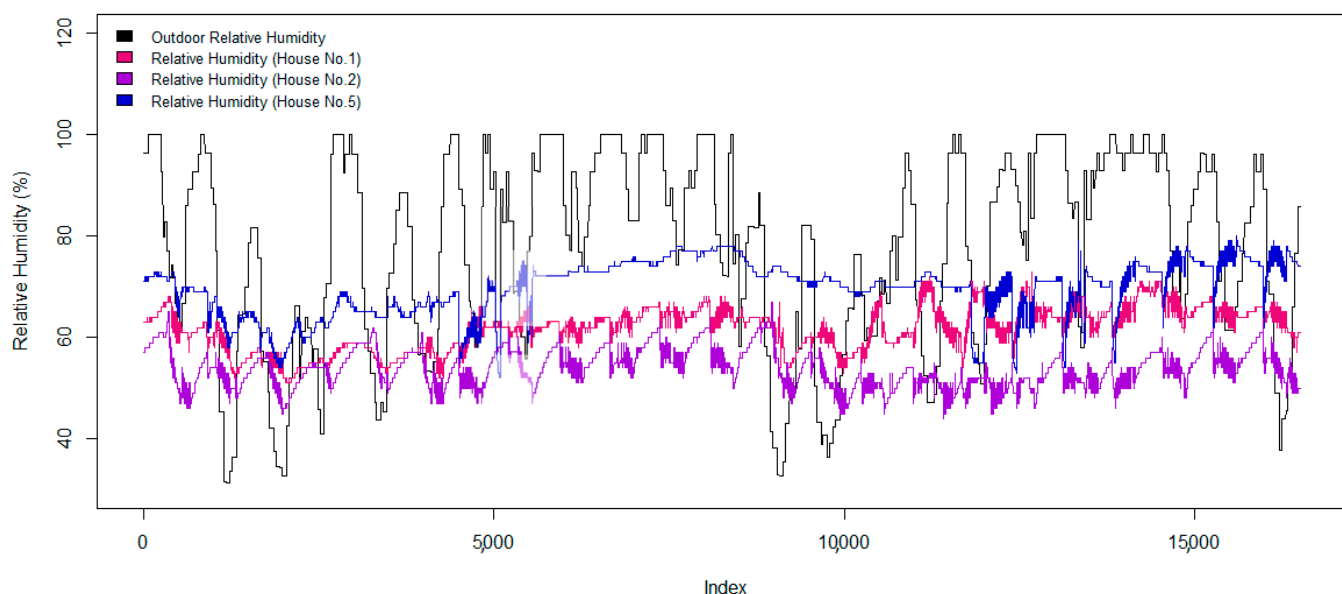

Figure 6. Actual outdoor relative humidity versus selected residences' relative humidity for the whole dataset.

Table 6. Savings from the implementation of thermal comfort control for the residences considered in study.

Model Savings/House No.	1	2	3	4	5
Temperature model only	40%	47%	46%	33%	40%
Relative humidity and temperature models	36%	42%	43%	29%	31%

5. Conclusions

The current work was on the prior work introduced by Lou et al. [13] and Alhamayani et al. [14]. In comparison, this study demonstrates a more realistic simulation of smart thermostat-based thermal comfort control in residences through consideration of a variable relative humidity. Greater accuracy was also achieved by using moving averages for the critical predictors (indoor temperature, indoor humidity, and cooling demand status). With improved accuracy models, the estimated cooling energy savings are more realistically predicted to be in the range of 29–43%, where the greater potential savings are achievable in residences with poor energy effectiveness.

The significance of this research is (1) that significant cooling energy and carbon savings could be achieved with virtually no cost and (2) that this approach could be used today in any residence with smart Wi-Fi thermostats to estimate savings from thermal comfort control. The next step has to be implementation of thermal comfort control at scale.

This work also has potential policy implications. As the smart Wi-Fi thermostat posed PMV thermal comfort control has a demonstrated potential to save energy and reduce carbon emissions at virtually no cost, it is reasonable to imagine policies emerging to set thermostat control standards based upon thermal comfort control. The establishment of standards for this would certainly be the domain of organizations such as ASHRAE in the US and REHVA in Europe. Of course, any standard emerging should not be draconian. Elderly people and people with health conditions may not be able to tolerate "stretch" PMV comfort levels to yield greater savings.

The limitations of this research are clearly seen. The shading and actual solar fenestrations can affect the developed MRT estimations accuracy. It is complex to figure out the time that a residence is shaded by a tree or surrounded residence. However, the study developed by Sun et al. [15] can be modified to let smart thermostats understand when the house is receiving solar irradiances or not, which could help this proposed technology overcome this limitation. Other limitations, such as the number and type of windows, can also be overcome by utilizing the same work done by Sun et al. [15] with knowledge of the total solar transmitted into the house and using in estimating the MRT value for the whole residence.

References

1. Masson-Delmotte, V.; Zhai, H.-O.P.; Pörtner, D.; Roberts, J.; Skea, P.R.; Shukla, A.; Pirani, W.; Moufouma-Okia, C.; Péan, R.; Pidcock, S.; et al. (Eds.) Summary for Policymakers. In *Global Warming of 1.5 °C. An IPCC Special Report on the Impacts of Global Warming of 1.5 °C above Pre-Industrial Levels and Related Global Greenhouse Gas Emission Pathways, in the Context of Strengthening the Global Response to the Threat of Climate Change, Sustainable Development, and Efforts to Eradicate Poverty*; IPCC: Geneva, Switzerland, 2018.
2. Dolf, G.; Ricardo, G.; Gayathri, P.; Rodrigo, L.; Rabea, F.; Ulrike, L.; Xavier, C.; Diala, H.; Bishal, P. *World Energy Transitions Outlook—1.5 °C Pathway*; International Renewable Energy Agency: Abu Dhabi, United Arab Emirates, 2021.
3. Dolf, G. *Global Energy Transformation—A Roadmap to 2050*; International Renewable Energy Agency: Abu Dhabi, United Arab Emirates, 2018.
4. New Report from Gemserv and Tado Shows Smart Thermostats Most Cost Effective and Scalable Way to Decarbonise Homes in the EU's Green Deal Renovation Wave. Business Wire. 21 October 2021. Available online: https://www.businesswire.com/news/home/20211021005179/en/New-Report-from-Gemserv-and-tado%C2%B0-Shows-Smart-Thermostats-Most-Cost-Effective-and-Scalable-Way-to-Decarbonise-Homes-in-the-EU%E2%80%99s-Green-Deal-Renovation-Wave (accessed on 4 February 2022).
5. Biden's Green Procurement Executive Order, Smart Thermostats, and More. Resources for the Future. Available online: https://www.resources.org/on-the-issues/bidens-green-procurement-executive-order-smart-thermostats-and-more/ (accessed on 4 February 2022).

6. Liu, J. Ownership of Smart Thermostat Reaches 13% in the U.S. The Comprehensive Security Industry Platform. Available online: https://www.asmag.com/showpost/26461.aspx (accessed on 22 January 2018).

7. Masoso, O.; Grobler, L.J. The dark side of occupants' behaviour on building energy use. *Energy Build.* **2010**, *42*, 173–177. [CrossRef]

8. Vakiloroaya, V.; Samali, B.; Fakhar, A.; Pishghadam, K. A review of different strategies for HVAC energy saving. *Energy Convers. Manag.* **2014**, *77*, 738–754. [CrossRef]

9. Ghahramani, A.; Dutta, K.; Yang, Z.; Ozcelik, G.; Becerik-Gerber, B. Quantifying the influence of temperature setpoints, building and system features on energy consumption. In Proceedings of the Winter Simulation Conference (WSC), Huntington Beach, CA, USA, 6–9 December 2015; IEEE: Piscataway, NJ, USA, 2015; pp. 1000–1011.

10. Ghahramani, A.; Dutta, K.B. Becerik-gerber, energy trade off analysis of optimized daily temperature setpoints. *J. Build. Eng.* **2018**, *19*, 584–591. [CrossRef]

11. Ferreira, P.; Ruano, A.; Silva, S.; Conceição, E. Neural networks based predictive control for thermal comfort and energy savings in public buildings. *Energy Build.* **2012**, *55*, 238–251. [CrossRef]

12. Danassis, P.; Siozios, K.; Korkas, C.; Soudris, D.; Kosmatopoulos, E. A low-complexity control mechanism targeting smart thermostats. *Energy Build.* **2017**, *139*, 340–350. [CrossRef]

13. Lou, R.; Hallinan, K.; Huang, K.; Reissman, T. Smart Wifi Thermostat-Enabled Thermal Comfort Control in Residences. *Sustainability* **2020**, *12*, 1919. [CrossRef]

14. Alhamayani, A.D.; Sun, Q.; Hallinan, K.P. Estimating Smart Wi-Fi Thermostat-Enabled Thermal Comfort Control Savings for Any Residence. *Clean Technol.* **2021**, *3*, 743–760. [CrossRef]

15. Sun, Q.; Alhamayani, A.; Huang, K.; Hao, L.; Hallinan, K.; Ghareeb, A. Smart Wi-Fi physics-informed thermostat enabled estimation of residential passive solar heat gain for any residence. *Energy Build.* **2022**, *261*, 111934. [CrossRef]

16. Smart Manufacturing Market. Market Research Firm. Available online: https://www.marketsandmarkets.com/Market-Reports/smart-manufacturing-market-105448439.html (accessed on 5 February 2022).

17. Fanger, P.O. *Thermal Comfort: Analysis and Applications in Environmental Engineering*; McGraw-Hill: New York, NY, USA, 1970.

18. American Society of Heating, Refrigerating and Air-Conditioning Engineers (ASHRAE). *Thermal Environmental Conditions for Human Occupancy, ANSI/ASHRAE Standard*; American Society of Heating, Refrigerating and Air-Conditioning Engineers, Inc.: Peachtree Corners, GA, USA, 2012.

19. Azuatalam, D.; Lee, W.-L.; de Nijs, F.; Liebman, A. Reinforcement learning for whole-building HVAC control and demand response. *Energy AI* **2020**, *2*, 100020. [CrossRef]

20. Park, J.; Kim, T.; Lee, C.-S. Development of Thermal Comfort-Based Controller and Potential Reduction of the Cooling Energy Consumption of a Residential Building in Kuwait. *Energies* **2019**, *12*, 3348. [CrossRef]

21. Li, Y.; De La Ree, J.; Gong, Y. The Smart Thermostat of HVAC Systems Based on PMV-PPD Model for Energy Efficiency and Demand Response. In Proceedings of the 2018 2nd IEEE Conference on Energy Internet and Energy System Integration (EI2), Beijing, China, 20–22 October 2018; pp. 1–6. [CrossRef]

22. Uğur, B.; Khalid, A.; Cihan, T. A comprehensive evaluation of the most suitable HVAC system for an industrial building by using a hybrid building energy simulation and multi criteria decision making framework. *J. Build. Eng.* **2021**, *37*, 102153. [CrossRef]

23. Huang, K.; Hallinan, K.; Lou, R.; Alanezi, A.; Alshatshati, S.; Sun, Q. Self-Learning Algorithm to Predict Indoor Temperature and Cooling Demand from Smart WiFi Thermostat in a Residential Building. *Sustainability* **2020**, *12*, 7110. [CrossRef]

24. Brownlee, J. Moving Average Smoothing for Data Preparation and Time Series Forecasting in Python. Machine Learning Mastery. 14 August 2020. Available online: https://machinelearningmastery.com/moving-average-smoothing-for-time-series-forecasting-python/ (accessed on 4 April 2022).

25. KumarI, A. Moving Average Method for Time-Series Forecasting. Data Analytics. 4 April 2021. Available online: https://vitalflux.com/moving-average-method-for-time-series-forecasting/ (accessed on 4 April 2022).

26. Xu, P.; Han, S.; Huang, H.; Qin, H. Redundant features removal for unsupervised spectral feature selection algorithms: An empirical study based on nonparametric sparse feature graph. *Int. J. Data Sci. Anal.* **2018**, *8*, 77–93. [CrossRef]

27. Hochreiter, S.; Schmidhuber, J. Long short-term memory. *Neural Comput.* **1997**, *9*, 1735–1780. [CrossRef] [PubMed]

28. Hu, Y.; Huber, A.E.; Anumula, J.; Liu, S. Overcoming the vanishing gradient problem in plain recurrent networks. *arXiv* **2018**, arXiv:1801.06105.

29. Corentin, T.; Yann, O. Can Recurrent Neural Networks Warp Time? Available online: https://arxiv.org/pdf/1804.11188.pdf (accessed on 5 February 2022).

30. Scott, W.; Thomas, P.; John, H.; Jonathan, L.R.; Les, A. Full-Capacity Unitary Recurrent Neural Networks. Available online: https://proceedings.neurips.cc/paper/2016/file/d9ff90f4000eacd3a6c9cb27f78994cf-Paper.pdf (accessed on 5 February 2022).

31. What Is PMV? What Is PPD? Basics of Thermal Comfort. SimScale. 14 June 2021. Available online: https://www.simscale.com/blog/2019/09/what-is-pmv-ppd/ (accessed on 5 February 2022).

32. Kingma, D.P.; Ba, J. Adam: A Method for Stochastic Optimization. Available online: https://arxiv.org/abs/1412.6980 (accessed on 5 February 2022).